Water Research 153 (2019) 324–334

Contents lists available at ScienceDirect

Water Research

journal homepage: www.elsevier.com/locate/watres

A cryogel-based bioreactor for water treatment applications

Dmitriy A. Berillo [a, *], Jonathan L. Caplin [b], Andrew B. Cundy [c], Irina N. Savina [a]

[a] School of Pharmacy and Biomolecular Sciences, University of Brighton, Brighton, UK
[b] School of Environment and Technology, University of Brighton, Brighton, UK
[c] School of Ocean and Earth Science, University of Southampton, Southampton, UK

ARTICLE INFO

Article history:
Received 8 October 2018
Received in revised form
12 January 2019
Accepted 19 January 2019
Available online 31 January 2019

Keywords:
Bacteria immobilisation
Bioremediation
Phenol
Cresol
Chlorophenols

ABSTRACT

The aim of this study was to develop and test a non-diffusion limited, high cell density bioreactor for biodegradation of various phenol derivatives. The bioreactor was obtained using a straightforward one-step preparation method using cryostructuration and direct cross-linking of bacteria into a 3D structured (sponge-like) macroporous cryogel composite material consisting of 11.6% (by mass) cells and 1.2–1.7% polymer, with approximately 87% water (in the material pores). The macroporous cryogel composite material, composed of live bacteria, has pore sizes in the range of 20–150 μm (confirmed by SEM and Laser Scanning Confocal Microscopy). The enzymatic activity of bacteria within the cryogel structure and the effect of freezing on the viability of the cross-linked cells was estimated by MTT assay. Cryogels based on Pseudomonas mendocina, Rhodococcus koreensis and Acinetobacter radioresistens were exploited for the effective bioremediation of phenol and m-cresol, and to a lesser extent 2-chlorophenol and 4-chlorophenol, utilising these phenolic contaminants in water as their only source of carbon. For evaluation of treatment scalability the bioreactors were prepared in plastic "Kaldnes" carriers to improve their mechanical properties and allow application in batch or fluidised bed water treatment modes.

1. Introduction

Bioremediation of contaminated water and soil is an effective approach for the removal of xenobiotics and other contaminants from the environment. It utilises the ability of microorganisms to degrade, or reduce the toxicity or mobility of, specific target compounds, and is considered one of the more efficient, cost effective and eco-friendly remediation methods. An extensive body of research has focused on utilising this method for a wide range of contaminants, including pesticides, heavy metals and aromatic hydrocarbons. For water treatment applications, the use of bacteria immobilised on a substrate has numerous advantages over the use of bacterial suspensions, such as higher biomass density, high metabolic activity, and higher resistance to toxic chemicals, allowing continuous operation processes (Villegas et al., 2016; Chen et al., 2007; Börner et al., 2014; Zaushitsyna et al., 2014; Gonzalez et al., 2001). Several bacterial immobilisation methods have been developed and various synthetic and natural carriers are known (Anku et al., 2017; Dzionek et al., 2016; Chiellini et al., 1999). The degree of bacterial immobilisation depends on the structure, pore size and surface area of the support, as well as the nature of the material (i.e. its hydrophobi-city, charge, etc.) and environmental conditions, such as pH, and temperature (Hailei et al., 2016; Cortez et al., 2017). Adsorption (to the substrate) or biofilm formation is often a long process however and represents the main cost, and one of the major limitations, of bioremediation using immobilised bacteria. Immobilisation methods via encapsulation of cells inside a polymer matrix (e.g. polyvinylalcohol (PVA), carrageenan and agar gel) can produce relatively high cell densities (Cortez et al., 2017; El-Naas et al., 2009; Sinha et al., 2011), however such materials tend to have diffusion limitations due to the use of high concentrations of polymer (6–10%) which coats the cells and restricts their interaction with contaminated water. Polyethylenimine(PEI) derivatives are a popular immobilising agent which have restricted application for bacterial immobilisation due to high toxicity issues (Virgen-Ortíz et al., 2017; Milović et al., 2005). In this study, we suggest a novel approach to the design of immobilised bacteria-based bioreactors for water treatment applications. To overcome existing limitations, a minimum concentration of polymers (1.2%) was used for cross-linking an 11.6% wt. suspension of bacterial cells in a 3D macroporous bacterial "sponge", produced via a facile one-step cryostructuration process. The morphology of the developed

* Corresponding author.
E-mail address: dmitriychemist@gmail.com (D.A. Berillo).

https://doi.org/10.1016/j.watres.2019.01.028

macroporous materials, based on *Acinetobacter radioresistens(Acn), Pseudomonas mendocina(Pse) and Rhodococcus koreensis(Rho)* with six commonly used immobilising polymers (and their combinations – PVA, PEI, chitosan, Gellan Gum and glutaraldehyde), was characterised and the materials tested for their bioremediation efficiency against phenol derivative compounds (phenol, *m-(p-)* cresols and CPs).

2. Materials and methods

2.1. Synthesis of aldehyde containing polymers

A combination of PVA-al and PEI-al was utilised as a cross-linking agent for bacteria (*Pse, Acn* and *Rho*). Polyvinyl alcohol was modified with aldehyde groups (PVA-al). Briefly, 0.6 mL of GA (50% v/v) was added to a 2% acidified PVA solution in distilled water. Note that the PVA modification is inefficient at neutral conditions. The reaction was terminated by pH adjustment to pH 6–7.5. Unreacted GA was removed by dialysis utilising a dialysis bag (cut off 12 kDa) against water. Polyethyleneimine (PEI) was modified in similar manner by adding 8.8 mL of GA (20 v/v %) to 2% polymer solution in water. The pH was adjusted to 7 prior to GA addition to avoid aldol condensation of aldehyde under alkaline conditions, and therefore to achieve a more consistent chemical composition of the polymer. The reaction mixture was incubated under stirring for 2h at room temperature, the pH adjusted to seven, and then the mixture was dialysed against water (a dialysis bag cut off 1 kDa). The obtained polymer solution was filtered through a 0.45μm membrane and stored at 4 °C until subsequent use. The concentration of the polymer in the solution was estimated by using a freeze drying method and measuring the final dry weight of the polymer.

2.2. Characterisation of polymers

FT-IR analysis of freeze dried polymers (PVA-al and PVA and PEI-al) was performed using a Bruker Alpha P instrument with attenuated total reflectance. Spectra were acquired in the 4000–400 cm^{-1} range with a resolution of 4 cm^{-1} for 24 scans to confirm the presence of aldehyde groups.

^1H NMR spectra of solutions of PEI-al and PVA-al (10 mg/mL) and non-modified PEI and PVA dissolved in D_2O were produced using a Bruker DSX 400 MHz spectrometer.

The molecular weight distribution of the modified polymers (PVA-al and PEI-al) was estimated via photon correlation spectroscopy, using a particle sizer (Zeta sizer 3000 HAS, Malvern Instruments Ltd., Malvern, Worcestershire, UK). Analysis was performed at 25 °C using a measurement angle of 90 °, with 11 runs for each measurement (n = 3). Zeta potential measurements of the polymers were also carried out (in triplicate) to estimate surface charge, using a Zeta sizer 3000 HAS (Malvern Instruments Ltd., Malvern, Worcestershire, UK, 1 mL aqueous dip cell, cuvette DTS1070 (n = 3)).

2.3. 3D macroporous bioreactor preparation

A significantly improved streamlined preparation method for 3D macroporous bioreactors (here termed cryobacteria reactors, or CBRs prepared within a special plastic carrier) is presented compared to one recently published by our group (Al-Jwaid et al., 2018). Briefly, 120 mL of media after cell cultivation OD_{600} 1.0–1.4 was centrifuged at 10 000 rpm for 10 min at 4 °C. According to literature data for *Pseudomonas sp.*, one unit OD_{600} corresponds to 2.08xE8 CFU and has a cell density of 2.085 mg/mL(Kim et al., 2012). The wet weight of the pelleted cells was calculated accordingly. For calculation of the bacterial cell density of *Rho* and *Acn* the following ratio was applied: an OD_{600} of one resulted in a cell wet weight of 1.7 g/L and 0.39 g/L of dry weight, respectively (Glazyrina et al., 2010). The pelleted cells (wet mass of 0.29g) were mixed gently with 2.5 mL of cross-linker solution in a phosphate buffer(PB) (pH 7.2) (or water or PB and 2% glucose) at various ratios (PEI-al-PVA-al 0.6:0.6% or 1.7% PVA-al), avoiding generation of bubbles in the cell suspension (all percentages shown in material compositions are based on % mass in the final composite material). This solution was transferred into a glass tube (diameter 9 mm) and frozen rapidly in a cryobath at −12 °C, and kept at that condition for 3 days. CBRs based on *Pse* (11.6%)-PVA-al-PEI-al 0.6:0.6% (Cryo-*Pse*), *Rho* (11.6%)-PVA-al-PEI-al 0.6:0.6% (Cryo-*Rho*), *Acn* (11.6%)-PVA-al-PEI-al 0.6:0.6% (Cryo-Acn) obtained were thawed at room temperature and used for bioremediation process testing directly.

Cryogels without bacteria were prepared according to the aforementioned procedure and were based on the combination of PVA-al-PEI-al 0.6:0.6% or PVA-al-PEI-al 1:1 and PVA-al 1.7%. These cryogels were used as a control to estimate nonspecific adsorption of phenol derivatives by the polymer matrix, and for physico-chemical characterisation.

Cryogels prepared from a combination of polymers PVA, PEI, chitosan(CHI), Gellan Gum(Gel) and glutaraldehyde(GA), as well as only GA(0.5%) and were prepared analogously to the above mentioned procedure. Prior to the addition of chitosan to the cells suspension, a stock solution was dissolved in 1% acetic acid. The stock solution of Gellan Gum (1.5%) was prepared in distilled water. CryoPho-PVA-PEI-GA 11.6:1:1:0.25%, CryoPho-PVA-PEI-GA 11.6:0.6:0.6:0.25%, CryoPho-CHI-GA 11.6:1:0.25%, CryoPho-Gel:PVA-al 11.6:0.3:1.0%, CryoPho-Gel:PVA-al 11.6:0.52:0.32%, CryoPho-Gel 11.6:0.5% CryoPse-Gel 11.6:0.5% were prepared at −12 °C and their bioremediation activity tested.

Cryobacteria reactors based on *Acn, Pse and Rho* were also prepared in polypropylene 'Kaldnes' carriers (d = 11 mm and h = 7 mm, with the volume of cell suspension 0.55 mL) using the same method as detailed above. Incorporation of the CBRs into plastic carriers improves their mechanical stability and decreases the possibility of mechanical damage under intensive mixing or application of high flow rate, or during the recharging of solutions between bioremediation cycles (Önnby et al., 2010; Rusten et al., 2006). CBRs based on: *Pse* (pellet of 100 mL, OD_{600} 1.06 or 221 mg), PVA-al-PEI-al 0.6:0.6% (CBR-*Pse*); *Rho (*pellet of 100 mL, OD_{600} 1.4 or 238 mg), PVA-al-PEI-al 0.6:0.6% (CBR-Rho); and *Acn* (adapted on the TSB plate to 2CP) (pellet of 100 mL, OD_{600} 1.04 or 170 mg) PVA-al-PEI-al 0.6:0.6% (CBR-Acn) were prepared in PB with final concentration of bacteria of 11.6%. The bacterial suspension was mixed with cross-linker and placed into a glass tube 11.5 mm in diameter containing plastic carriers. The glass tube was frozen at −12 °C for 3 days. Then CBR samples in the carrier (*Pse* PVA-al-PEI-al 11.6:0.6:0.6% (CBR-*Pse*) (44 mg of cells/carrier), *Rho*-PVA-al-PEI-al 11.6:0.6:0.6% (CBR-*Rho*) (47.6 mg of cells/carrier), and *Acn*-PVA-al-PEI-al 11.6:0.6:0.6% (CBR-*Acn*) (34 mg of cells/carrier)) were thawed at room temperature and used for bioremediation process testing directly.

The number of live bacteria in the CBRs was assessed using a MTT assay (Hao et al., 2002), following standard methods.

2.4. 3D macroporous bioreactor characterisation

The elastic moduli of the cryogel bacteria reactors (CBRs) were studied using a TA-XT2 instrument (Stable Micro Systems, Godalming, Surrey, UK). The compression test was performed at room temperature. The cryogels were prepared with a diameter of 8 mm and height of 9 mm. Samples were compressed up to a deformation level of 50% at a speed of 0.05 mm/s. The elastic modulus was

calculated at a deformation of 5% using the equation

$$E = (F/S)/(\Delta h/h)$$

where E is the elastic modulus (Pa), F is the force applied (N), S is the cross-sectional area of the sample (m^2), Δh is the height (m) at compression, and h is the original height (m) (Kirsebom et al., 2013).

Three samples were used for each type of composite cryogel.

Scanning electronic microscopy (SEM) images were obtained using a Zeiss Sigma field emission gun SEM (Zeiss NTS). Slices of CBRs with thickness of 1–2 mm were washed with PBS, and then samples were fixed in 5% v/v GA in PBS overnight following by washing with PBS and water. Then, slices were frozen at −20 °C overnight and freeze dried in a Christ ALPHA 2–4 freeze-dryer for 24 h. Finally, freeze-dried samples were coated with a layer of platinum using a Quorum (Q150TES) coater.

Confocal laser scan microscopy (CLSM) images were obtained using a Leica TCS SP5 using objective lens x10, x20, x40 and x63. CBRs were fixed in 5 v/v % GA in PBS buffer overnight and then cut into slices with a thickness of 1 mm. Samples were washed with distilled water to remove non-crosslinked bacteria and stained with Rhodamine B solution overnight. Unbound Rhodamine B was washed out with water. Another batch of CBRs was stained with FITC solution (0.02 mg/mL in sodium phosphate buffer, pH 9.0) overnight. Non-reacted FITC was washed out with water. The 488 and 530 nm excitation and emission wavelengths were applied. Images were produced by optical sectioning in the xy-planes along the z-axis with 30–70 optical sections with 1 μm intervals.

Evaluation of the viability of crosslinked bacteria within the cryogel was performed using standard Live/Dead assay. Cryogels were cut into thin slices with a thickness of 1 mm and washed out with NaCl 0.9% solution to remove uncross-linked cells. Samples were stained using Live/Dead Bac Light kit containing SYTO 9 stain at wavelength 480/500 nm and propidium iodide at wavelength 490/635 nm for 15 min at room temperature under dark conditions (according to the protocol of the LIVE/DEAD ® Bacterial viability kit of staining).

2.5. Bioremediation by suspensions of bacteria and CBRs

The degradation of phenol, *m*-cresol and 2-chlorophenol (2-CP) or 4-chlorophenol (4-CP) by a suspension of non-crosslinked bacteria and by various CBRs was studied. In the case of bioremediation by a bacterial suspension(planktonic state) the same amount of bacteria (measured based on OD_{600}) as applied in the cryogel preparation was used. Forty mL of phenol derivative were added to the pellet of bacteria in a sterile 50 mL plastic falcon tube. The tube was regularly opened for sampling (207 μL at each time point) under sterile conditions. Note that the tube contained approximately 10 mL of air. The tubes were shaken at 150 rpm at 30 °C in the dark(dynamic mode). The number of bacteria in the solution during the bioremediation process was monitored by measurement of OD_{600} at each sampling point.

CBRs were placed in 40 mL of phenol derivative (phenol, m-cresol, 2-CP and 4-CP) in minimum salt media (MSM) buffer at pH 7.0 in a static mode(without additional shaking) at 30 °C. Control sterile solutions (phenol, m-cresol, 2-CP and 4-CP in MSM) were prepared under the same conditions and tested to estimate stability against degradation over time in a static mode. Nonspecific adsorption of 4-CP on the PEI-al-PVA-al and PVA-al control cryogels (without bacteria, see section 2.3) was evaluated in MSM at 30 °C in dymanic mode. Due to observable biofilm formation in the glass bottle during the bioremediation process, each cycle was performed in a new set of sterile bottles to eliminate the effect of biofilm formation on the following bioremediation cycles. The efficiency of the bioreactors was calculated as previously discussed (Börner et al., 2014), based on the change of contaminant concentration at a given time point (48 and 220h) divided by the experimental duration (i.e. the number of hours of bioreactor or bacteria exposure to the target contaminant) (mg/L/h) according to the equation: Efficiency=$(C_0\text{-}C_t)$/t.where C_0 is initial concentration, C_t concentration at a time point.

The error was calculated according to the standard equation:

Error = (StDev(A1:Ai))/($\sqrt{}$(COUNT(A1:Ai))), where StDev is standard deviation, COUNT(A1:Ai) number of replicates

3. Results and discussion

3.1. Cryobacteria reactor (CBR) preparation and characterisation

In our recent work we used combinations of polymers GA(0.385%); GA & PVA (0.385:0.77%); PVA-al & PEI-al(0.385:0.46%); PVA-al & PEI-al(0.77:0.19%), keeping the concentration of bacteria at 23% (by mass) for preparation of cryogels (Al-Jwaid et al., 2018). Here, to select the best performing bioremediation system, cryobacteria reactors based on three bacterial strains and six immobilising polymers (and their combinations) were screened. PVA and PEI modified with aldehyde groups were used as cross-linkers. The presence of aldehyde group in the modified polymers was confirmed by FTIR and ^{1}H NMR spectroscopy (Figs. S2(a–c)). As expected the zeta potentials of the PVA and PVA-al were close to zero, illustrating the electroneutrality of the cross-linking agent, whereas PEI-al showed a zeta potential of 32 ± 4 mV indicating that the cross-linker is positively charged (Fig. S3) and therefore can additionally interact with cell membranes via electrostatic interactions. Additionally, cryogels with chitosan and Gellan Gum were prepared to analyse the bacteria immobilisation as result of electrostatic interaction between the cell membrane and these polymers.

In previous work, bacteria capable of the bioremediation of phenol were immobilised on cryogel surfaces in three steps; overall the cryogel preparation and the following biofilm formation was completed in 10 days and required the use of additional equipment such as UV lamps (400 W) (Satchanska et al., 2015). The subsequent bioreactor contained a large amount of bulk polymer leading to issues of disposal after its use, and this technique therefore is less practical for industrial application.

Here, suspensions of *P. mendocina (Pse), R. koreensis (Rho)* and *A. radioresistens (Acn)* (*11.6 w/w%)* were cross-linked by a combination of PEI-al-PVA-al (0.6–0.6 w/w%) prepared in PB in a one-step cryostructuration process. When the suspension of cells and cross-linker freezes under semi-frozen conditions (−12 °C) ice crystals form, which leads to phase separation of the cells and the cross-linker suspension and ice (Fig. 1). The growing ice crystals expel all solutes and bacteria into a non-frozen liquid microphase, which remains non-frozen even at −12 °C (Kirsebom et al., 2013). The bacteria and cross-linker therefore concentrate in the thin non-frozen liquid microphase, and the bacteria become densely packed and cross-linked by functional polymers interacting with their cell membranes. Thawing of samples results in the melting of the ice crystals, producing water-filled voids - pores. This results in a 3D structured macroporous material, formed in a one-step preparation method, with the pore walls composed mostly of bacterial cells tightly attached to each other, surrounding a well-developed system of interconnected large pores with size 20–150 μm (Fig. 2). The obtained cryogels were self-supporting, mechanically stable

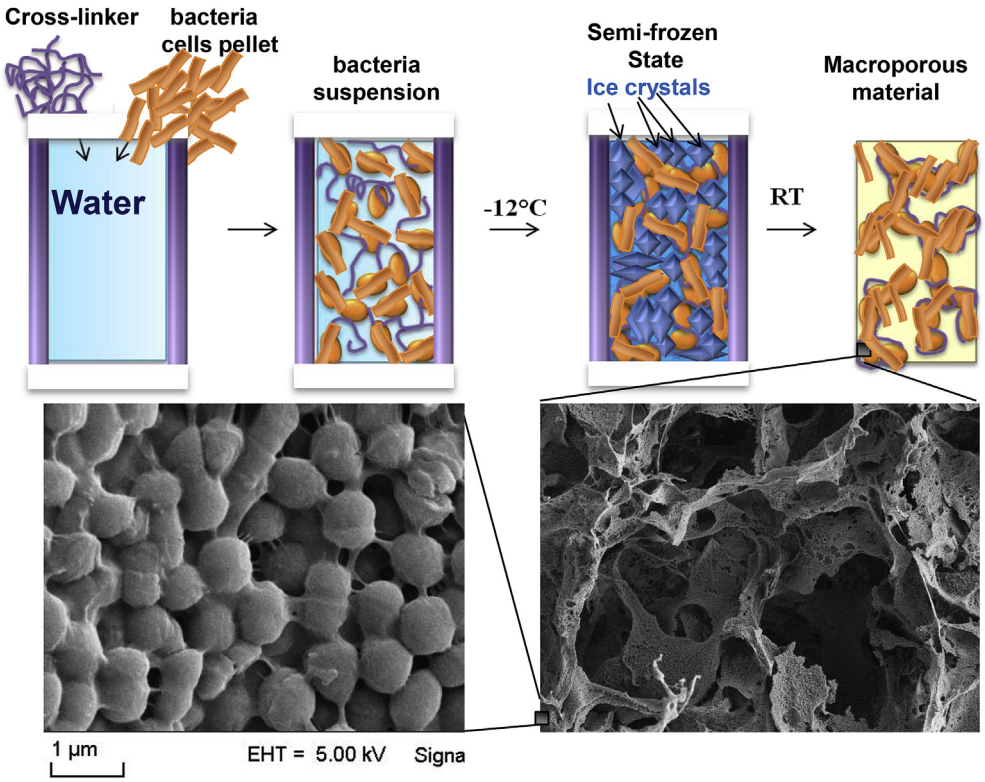

Fig. 1. Scheme of cryobacteria reactor (CBR) preparation and the morphology and texture of the material based on *Rhodococcus sp*.

(Fig. S4), and withstand processing in a static and a dynamic mode (i.e. shaking at 150 rpm) for at least 4 weeks (Fig. S5(A-D)).

Rapid aggregation of cells was observed upon addition of glutaraldehyde. The Cryo-*Acn*-PVA-al has no obvious cells in the cryogel wall due to use of a relatively high concentration of cross-linking agent (1.7%, Fig. 2i(A-C)). It was observed that the change of composition of the buffer did not change the morphology of the material significantly (Fig. 2ii). Nevertheless, the use of PB or PB & glucose has advantages compared to cryogels prepared in pure water, as these decrease the osmotic stress during cryogel preparation and keep the pH constant.

To visualise the efficiency of mixing of the bacteria with the polymer, as well as to assess the distribution and amount of live cells, CBRs were stained with Live/Dead stains. The hydrogel based on Gellan was characterised by the absence of large pores in the structure of the composite hydrogels, and a homogeneous distribution of cells within the material (Fig. 3(E-H)). A strong fluorescence background due to electrostatic binding of the positively charged dyes with the negatively charged polymer can be observed under CLSM. Nevertheless, at magnification x100 the images clearly distinguish between cells and background (Fig. 3H). The material has a predominantly microporous structure however and therefore can be used only in batch application in a dynamic mode (Fig. 3E-H). We focused on preparation and assessment of the bioremediation activity of macroporous materials, which potentially could be used additionally in a flow through mode.

Some of the key beneficial properties of cryogels relate to their elastic strength, flexibility and shape recovery. In our recent study we comprehensively investigated the rheological properties of cryogels based on bacteria (Al-Jwaid et al., 2018), however the elastic modulus was not measured. The elastic modulus of the cryogels *Acn*-PVA-al (1.0%) and *Acn*-PVA-al-PEI-al (1.0:0.25(%)) was 3.52 ± 0.7 and 4.64 ± 0.1 kPa, respectively. These values were similar to those previously reported for cryogels made of *E. coli* and activated polyethylenimine, which had an elastic modulus of 3.1 ± 0.39 kPa (Zaushitsyna et al., 2014), or porous material *C. saccharolyticus* cross-linked by glutaraldehyde which showed a modulus in the range 8–29 kPa (Kirsebom et al., 2009). Our data were also comparable with the elastic modulus of cryogels based on polymers such as enzymatically cross-linked casein (1.3–7 kPa) and gelatin (0.95–1.9 kPa) (Kirsebom et al., 2013) or combinations of polymeric cross-linking agent aldehyde dextran and gelatin (0.6–2.8 kPa), respectively (Berillo and Volkova, 2014). Cryo-Rho-PVA-al-PEI-al-Gel (11.6:0.5:0.6:0.3(%)), Cryo-Rho-PVA-al-Gel (11.6:1.0:0.3(%)) prepared in water, and Cryo-Rho-PVA-al-Gel (11.6:1.0:0.3(%)) formed in phosphate buffer had elastic moduli of 16.1 ± 1.7, 87.7 ± 16.3, 28.7 ± 17.0 kPa, respectively. As expected, an increase of CHI concentration from 0.5 to 1.0% at constant polymer cross-linking mass ratio (2:1) led to a significant increase in the toughness of the material (Fig. S4). Cryogels based on *Rho(*11.6%) in combination with polymers CHI-GA 0.5:0.25% and CHI-GA 1.0:0.5%, PEI-GA1.0:0.25%, and 1.0:0.5%, PEI-PVA-GA 1.0:1.0:0.25% showed an elastic modulus of 34.7 ± 15.5; 1955 ± 268; 12.4 ± 8; 10.8 ± 0 .9; 7.2 ± 1.5 kPa, respectively. As expected the highest elasticity modulus was found for samples based on CHI, which is related to the rigid structure of this polysaccharide. The incorporation of Gel to the structure significantly improves the mechanical properties of the material due to formation of a physical gel. In Fig. S4 an illustrated comparison of the elastic properties of composite cryogels based on *Rhodococcus sp* is given.

The analysis of live and dead bacteria using live/dead kit indicates that most of the bacteria after cross-linking were viable (stained green, Fig. 3e-h) even after undergoing freeze-thawing conditions during the cryogelation process. Potentially, cryogenic conditions (particularly ice-crystal formation) as well as the cross-linker and the osmotic stress itself could damage the bacterial cells

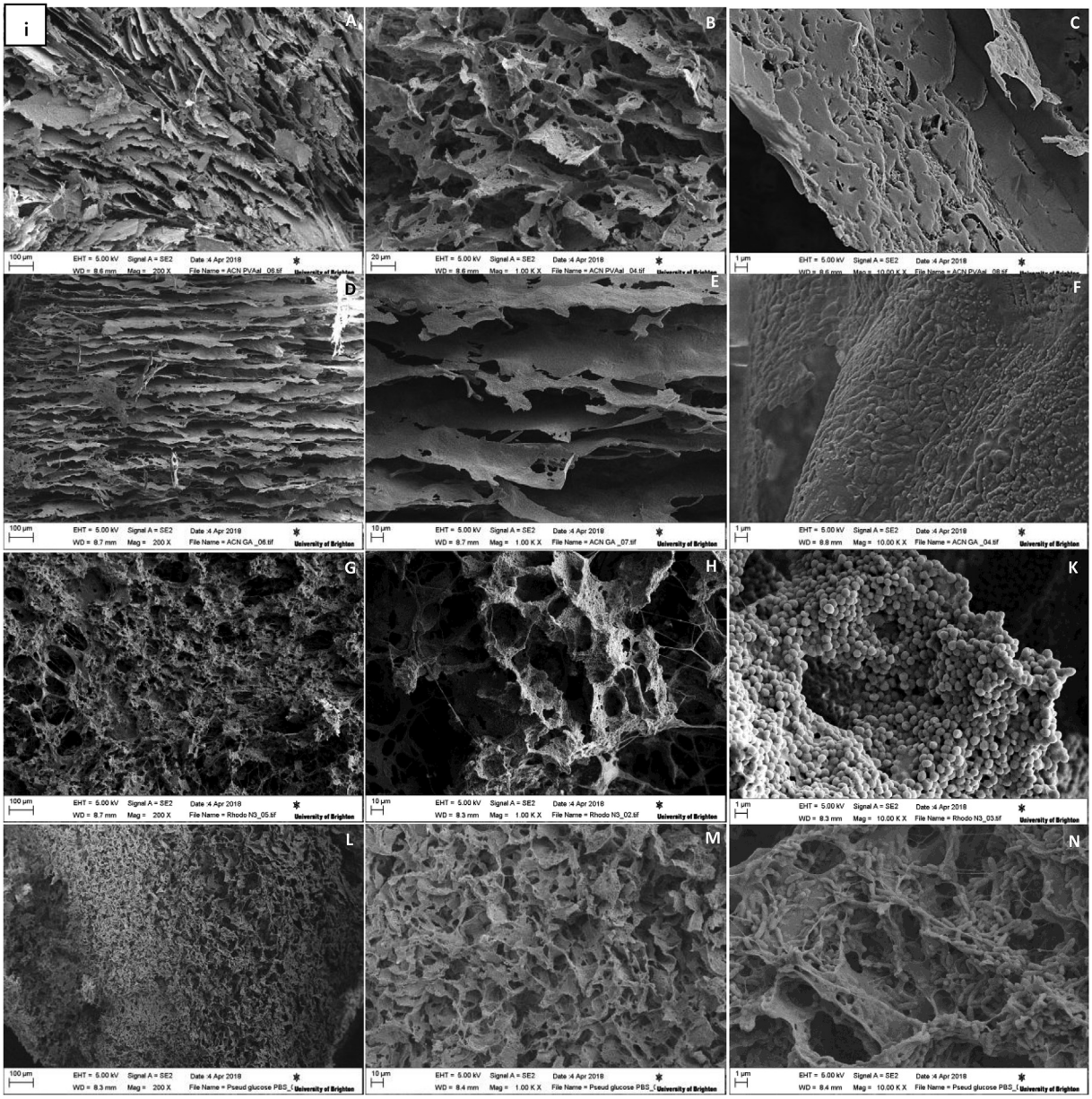

Fig. 2. SEM images of cryogels: i) Cryo-Acn-PVAal(A-C), Cryo-Acn-GA(D-F), Cryo-Rho-PVA-al-PEI-al(G-K) and Cryo-Pse-PVAal-PEI-al(L-N) at 200x, 1000x and 10000 magnifications; ii) Cryo-Rho-PVA-al-PEI-al prepared in: a) water; b) phosphate buffer; c) phosphate buffer and 1% glucose; Cryo-Pse-PVAal-PEI-al: d) in water; e) phosphate buffer; f) Cryo-Acn-GA(0.5%) at 30 000 times magnification.

and reduce viable cell numbers. To distinguish the potential harmful effects of the polymer cross-linker from those caused by cryogenic conditions the experiments were performed at 4 °C/ −12 °C, respectively. Incubation of *Rho* suspension in the solution of PBS containing 0.25 or 0.5% of GA (negative control) at 4 °C for 24 h led to a significant decrease in the number of live bacteria, to 27% and 22% of initial numbers respectively, due to the toxicity of GA. The use of PEI-al (0.365 w/v %) in PBS resulted in a 25% of live *Acn* bacteria. PEI-al was more toxic compared to unmodified PEI (where 50% of bacteria survived). PVA-al 1.2% in PBS buffer at 4 °C revealed a high survival of *Acn* (92.4%) compared to a bacterial suspension stored in phosphate buffer without polymer (100%) (positive control) (Table S1).

The issue of the relatively high toxicity of PEI-al was overcome by the use of a combination of nontoxic PVA-al with PEI-al, leading to 72.5% active bacteria. The use of only PVA-al led to formation of a material with low water permeability, while using a combination of PVA-al-PEI-al (1:1) resulted in formation of a material with desirable porosity characteristics and mechanical properties. A small amount of glucose, which acted as a cryoprotector and potentially as a source of carbon, was added to the bacterial suspension to decrease the effect of cell bacteria damage due to ice crystal formation and osmotic shock (Moslemy et al., 2002). PVA-al 1.2% dissolved in PBS buffer in the presence of 2% glucose showed some growth of the *Acn* bacteria at 4 °C (109%) after 24h (Table S1). The frozen suspension of *Acn* in PVA-al 1.2% and PBS buffer with 2% glucose added showed 88.6% survival from the initial number of cells. Thus, a decrease of 11.4% in live bacteria was related to bacterial damage by growing ice crystals. The effect of 1.0% glucose in PBS buffer on bacterial viability was also investigated (Table S1). The incubation of *Pse* suspension in PBS buffer containing 1.0% glucose over 24 h at 4 °C led to a 13.8% decrease in cell populations

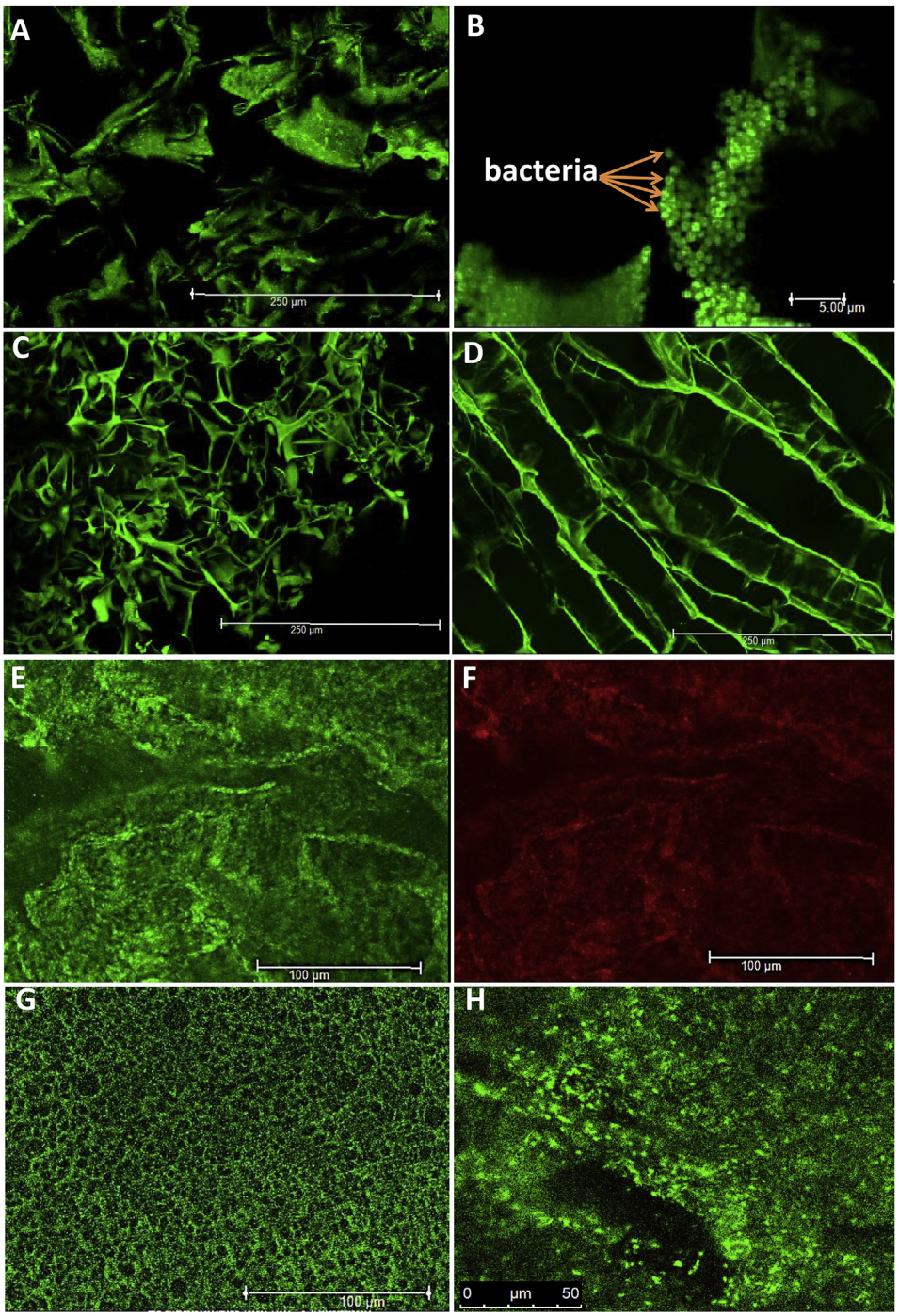

Fig. 3. CLSM images of Cryo-Rho (green colour illustrates fluorescence of bacteria stained in fluorescent dye, black background corresponds to the empty voids pore structure) at x times magnification: A) x 20 (scale bar 250 μm), B) x170 (scale bar 5 μm), C) Cryo-Rho-PEI-GA(1.0%:0.25%); D) cryo-Rho-CHI-GA(1.0:0.25%), x 20 (scale bar 250 μm); Hydrogels stained with Live/Dead kit: (green colour illustrates fluorescence of live bacteria, red background corresponds to dead bacteria): E) hydrogel-Rho-Gel (0.5%) illustrating fluorescence of viable cells, F) hydrogel-Rho-Gel(0.5%) illustrating fluorescence of dead cells; G) Cryo-Rho-Gel(1.0%) at x63 times magnification (scale bar 100 μm) and H) Cryo-Rho-Gel-PVA-al(0.5%:0.3%) at x100 times magnification (scale bar 50 μm). (For interpretation of the references to colour in this figure legend, the reader is referred to the Web version of this article.)

compared to the PBS buffer. The presence of glucose did not significantly improve the viability of *Pse* during the cryogelation process either (Table S1). It can be concluded that addition of glucose in combination with PVA-al-PEI-al (1:1) did not significantly improve the survival of the bacteria or even had some negative effect on *Pse*, but conversely it had a positive effect on *Acn* during incubation for 24 h at 4 °C. It can also be concluded that the 23% *Pse* bacteria population decrease observed after incubation at 4 °C for 24h was due to cumulative toxicity from the PVA-al-PEI-al polymers, while the 53% loss of bacteria after cryogelation was presumably due to damage of the bacteria by growing ice crystals during the cryo-structuration process (Table S1).

3.2. Bioremediation of phenol and cresols

Recently we illustrated the bioremediation efficiency of cryogels based on *Pse, Rho* and a *Pse:Rho* mixture for 50 ppm phenol in carbonate buffer in a dynamic mode (Al-Jwaid et al., 2018). In this study phenol and m-cresol bioremediation by Cryo-*Rho*, Cryo-*Pse*, and Cryo-*Acn* cryogels was examined in dynamic and static mode in MSM buffer (50 ppm (40 mL) and compared with bacterial suspensions (Fig. S5(D) and S6). Suspensions of bacteria of *Pse* or *Acn* degraded 50 ppm (40 mL) of phenol in 7 days (166h), whereas *Rho* completed the degradation in 9 days (220h) (Fig. S5(D)). Increasing the phenol concentration to 100 ppm resulted in 39.5% phenol degradation by a suspension of *Acn* over 220h (bioremediation efficiency 0.123 mg/L/h). *Rho* formed a biofilm on the glass surface in the solution of phenol (100 ppm, 200 mL), and did not degrade phenol over 12 days of incubation (data not shown).

CBR-*Pse*, CBR-*Acn* and CBR-*Rho* were more efficient for phenol degradation compared to a suspension of equivalent bacteria (Table 1). Bacterial suspensions of *Pse* or *Acn* degraded 50 ppm (40 mL) phenol in 166h, whereas *Rho* completed the degradation in 220h (Fig. S5(C)). Cryogel *Pse*-Gel (0.5%) showed slow bioremediation of m-cresol (300 ppm), with 21% degraded over 17 days in a static mode. The presence of polysaccharide Gel in the structure of the cryogel decreased the bioremediation efficiency of the material, which might be related to its consumption as a source of carbon. A cryogel composed of a combination of *Rho*, 0.13% of PVA-al and 0.5% Gel was not as effective for phenol bioremediation as cryo-*Rho* PVA-al-Gel (1.0:0.3%) (Fig. 4A). Other polymer compositions were used for cryogels preparation based on PEI-PVA-GA(1:1:0.25%); PEI-PVA-GA(0.6:0.5:0.25%), CHI-GA(1:0.25%) (Fig. 4B), which revealed complete bioremediation of m-cresol (50 ppm) in 116 and 225h, respectively.

The suspension of bacteria *Acn* produced only 10% degradation of m-cresol (50 ppm, 200 mL, a static mode) within 12 days. There was no significant difference in *m*-cresol biodegradation by *Pse* and *Rho*. The suspension of *Rho* degraded only 11% of m-cresol (50 ppm, 200 mL) after 12 days (data not shown). The first bioremediation cycle of m-cresol (50 ppm, 200 mL) by CBR-*Acn* (9×10^6 CFU) was completed within 5 days. The addition of fresh phenol solution (100 ppm, 200 mL) to the CBR-*Acn* instead of *m*-cresol resulted in only 50% consumption of phenol within 8 days, indicating that the same batch of CBR-*Acn* might be utilised for bioremediation of mixed or complex mixtures, but with similar (by structure) contaminants, i.e. it can be acclimatised to a new contaminant, however it took a longer time compared to the model system(Fig. 4C).

The bioremediation of the *m*-cresol was slower over the first 90h of testing for the three bacteria cryogels of cryo-Rho-PEI-PVA-GA, cryo-Rho-PEI-PVA-GA and cryo-Rho-CHI-GA due to bacterial acclimatisation prior to *m*-cresol consumption (Fig. 4B). Bioremediation with CBR-*Rho* and CBR-*Pse* consumed 71% of *m*-cresol (40 mL, 50 ppm) after 10 days (Fig. 4C). The bioremediation using CBR-Rho at higher *m*-cresol concentrations (40 mL, 100 ppm) indicated only a 30% decrease in *m*-cresol concentration(data is not shown). CBR-*Acn* revealed better ability to degrade m-cresol compared to CBR-*Rho* and CBR-*Pse*. The 1st, 2nd and 3rd bioremediation cycles *of m*-cresol (50 ppm) by CBR-*Acn* were completed within 265, 90 and 46h, respectively. Regardless of which bacterial strains were used (*Pse, Rho* and *Acn*), the CBR had an adaptation period to phenol and m-cresol of 48h and 90h, respectively. CBR-*Acn* showed the best degradation efficiency for *m*-cresol among the studied bacterial strains.

Following this, the bioremediation process was scaled up in a static mode, and the volume of the solution was increased to 200 mL, revealing a significant decrease of concentration within 100–120h for the studied bacterial strains (Fig. 5). The biodegradation of phenol by CBR-*Pse*, CBR-*Rho* and CBR-*Acn* was studied with addition of a fresh portion of phenol after each bioremediation cycle. CBR-*Pse* and CBR-*Acn* consumed 60 ppm of phenol within 200h whereas CBR-Rho completed the bioremediation in approximately 100h for the first cycle. It is important to note that CBR-*Pse*, CBR-*Rho* and CBR-*Acn* revealed similar phenol degradation activity for following 2–10 cycles, which were complited within approximately 60–65h (Fig. S6(A-C)). To the best of our knowledge there is still no information about the efficiency of *Rho* to degrade phenol, cresols and chlorophenols. *Pseudomonas spp.* has been previously used for bioremediation of benzene and toluene into phenol and cresol (Tao et al., 2004, 2005). Calculation of degradation efficiency showed that CBR-*Pse* caused a more rapid bioremediation of phenol compared to CBR-*Rho* or CBR-*Acn* (Fig. 5 and Table 1). CBR-*Rho* needed an acclimatisation period of approximately 48h before the bacteria became active for bioremediation. CBR-*Pse*, CBR-*Acn* and CBR-*Rho* were more efficient for phenol degradation compared to a

Table 1
Bioremediation efficiency (mg/L/h) of cryogels(1 mL) and suspensions of bacteria *Pse, Rho* and *Acn* for Phenol(Ph), m-cresol and 4CP for the 1st cycle otherwise specified, volume of solution 40 mL otherwise specified.

CBRs prepared within plastic carriers	Bioremediation efficiency, mg/L/h		
	CBR-*Rho*	CBR-*Pse*	CBR-*Acn*
Cresol 50 ppm at 48h	0.0964 ± 0.029	0.234 ± 0.019	0.307 ± 0.064
Cresol 50 ppm at 220h	0.166 ± 0.051	0.535 ± 0.125	0.60 ± 0.10
Ph 100 ppm at 48h, 2nd cycle	2.18 ± 0.15	2.250 ± 0.166	0.761 ± 0.098
Ph 100 ppm at 48h, 3rd cycle	1.84 ± 0.089	–	1.860 ± 0.240
Ph 50 ppm at 48h (V 200 mL)	0.091 ± 0.021	0.60 ± 0.10	0.363 ± 0.0424
Ph 50 ppm at 120h (V 200 mL)	0.468 ± 0.007	0.50 ± 0.01	0.517 ± 0.016
Free suspensions of bacteria	*Rho* suspension	*Pse* suspension	*Acn* suspension
Cresol 50 ppm at 120h (V 200 mL)	0.0074	–	0.068 ± 0.073
Phenol 50 ppm at 48h	0.028 ± 0.003	0.159 ± 0.080	0.42 ± 0.080
Phenol 50 ppm at 120h	0.213 ± 0.045	0.317 ± 0.080	0.352 ± 0.050
Phenol100 ppm at 48h, 2nd cycle	0.048 ± 0.039	–	0.276 ± 0.044
Phenol 100 ppm at 120h 2nd cycle	0.039 ± 0.011[d]	–	0.184 ± 0.026
CBRs without plastic carriers	Cryo-*Rho*	Cryo-*Pse*	Cryo-*Acn*
Cresol 50 ppm at 48h (V 200 mL)	0.086 ± 0.022	0.386 ± 0.086	0.0833 ± 0.099
Phenol 50 ppm at 48h	0.371 ± 0.022	0.151 ± 0.020	–
Phenol 50 ppm at 120h	0.874 ± 7xE-4	0.237 ± 0.050	–
4CP 50 ppm at 48h	–	0.333 ± 0.038	–

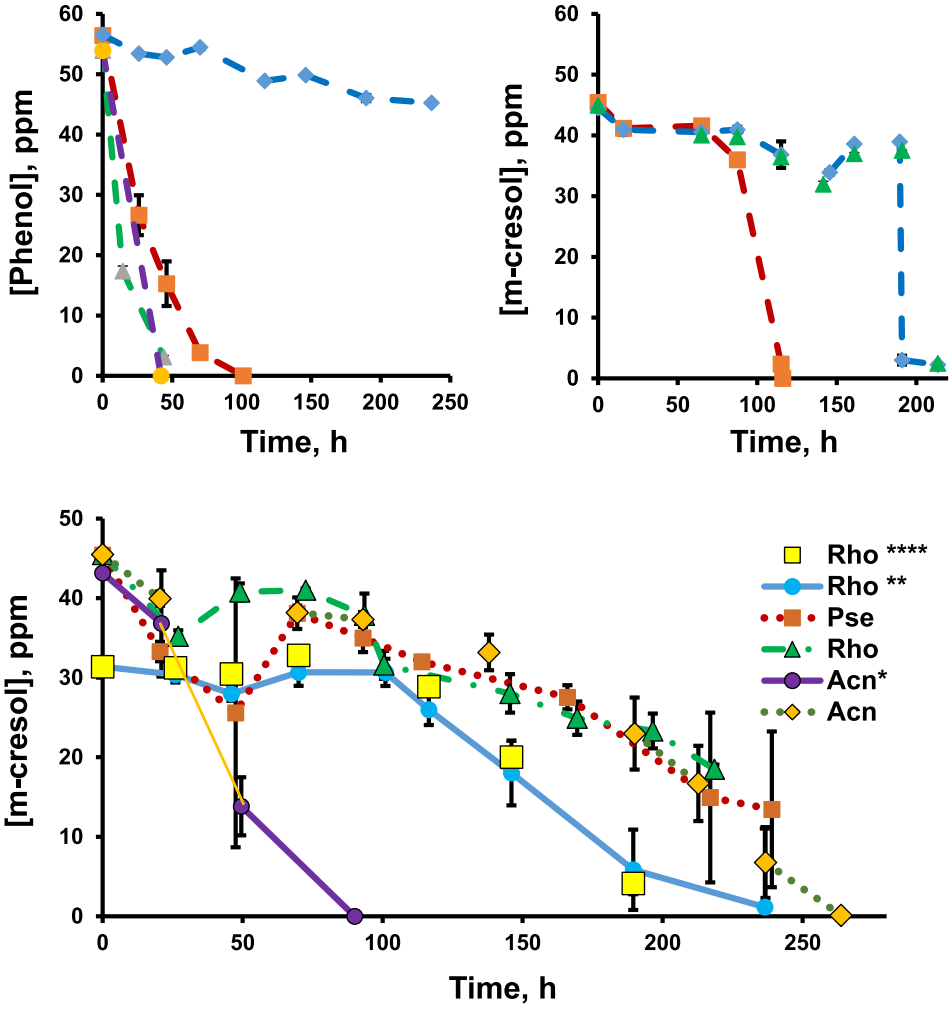

Fig. 4. Degradation of phenol derivatives by cryogel made of: **A)** cryo-*Rho*-Gel-PVA-al (11.6:0.52::0.13%) (◆); cryo-*Rho*-Gel-PVA-al (11.6:0.3:1.0%) 1st cycle (■); cryo-Rho-Gel-PVA-al (11.6:0.3:1.0%), 2nd cycle(▲); cryo-*Rho*-Gel-PVA-al (11.6:0.3:1.0%), 3rd cycle(●), 40 mL of 50 ppm phenol. **B)** cryo-Rho-PEI-PVA-GA (11.6:0.6:0.5:0.25%) (◆); cryo-Rho-PEI-PVA-GA (11.6:1.0:1.0:0.25%)(■); cryo-Rho-CHI-GA (11.6:1.0:0.25%) (▲), 40 mL of 50 ppm m-cresol. **C)** CBR-*Rho*(within plastic carrier) ($12.24 \pm 3.6 \times 10^6$ CFU, 40 mL) and CBR-*Pse* and CBR-*Acn*(within plastic carrier) ($39.69 \pm 1.4 \times 10^6$ CFU, 200 mL) for 1st cycle, 40 mL of 50 ppm m-cresol; *2nd bioremediation cycle, **Cryo-*Rho*-PEIal-PVAal, ****Cryo-*Rho*-PVA-al.

suspension of equivalent bacteria (Table 1) and phenol bioremediation efficiencies were 0.6, 0.363 and 0.0915 mg/L/h (48h), respectively (Fig. 5). It can be concluded that the selected strains *Pse*, *Rho* and *Acn* preferably degrade phenol while the biodegradation of m-cresol took place at least 3 times more slowly (Fig. 4C).

Overall, the CBRs show resistance to high concentrations of phenol derivatives and significantly faster bioremediation (Fig. 5 & Fig. S5(A-C)) compared to equivalent suspensions of bacteria in a static mode (Fig. S5(D)). Moreover, the recovery of the bioreactors is straightforward and does not require centrifugation to separate suspensions of bacteria from the aqueous solution, making the whole bioremediation process considerably simpler to apply. The same CBR-*Pse*, CBR-*Rho*, CBR-*Acn* biorectors were used over 10 bioremediation cycles without showing any decline in activity over more than one month of exploitation, demonstrating the ability for reuse of the material over repeat cycles (Fig. S5(A-C)).

As noted above, suspensions of bacteria cannot be used instantly for bioremediation of high phenol concentrations (>60 ppm). An increase in phenol concentration resulted in prolongation of the bioremediation process required for its complete degradation (Fig. 5A-C). There was no delay of bioremediation at high concentrations of contaminant for the 2nd (and following) bioremediation cycles. MTT assay after 17 days of the bioremediation process showed, for CBR-*Pse*, a significant increase in bacterial numbers compared to initial numbers (Table 2), indicating their existence in an exponential growth phase. In contrast, CBR-*Acn* and CBR-Rho showed a decrease in bacterial numbers following treatment (Table 2) indicating that these bacteria had entered a senescence phase. Based on Fig. 5 one can assume that 300 ppm is not the limit for the bioremediation process, however there are few examples where such high concentrations would be encountered in a real case scenario therefore higher phenol concentrations were not tested further. Usually the concentration of phenols in waste water is quite low and adaptation of the CBR is unnecessary, but in cases where faster bioremediation of high concentrations of phenols (200–300 ppm) is required, CBRs may be pre-adapted to phenol at concentrations of 25–50 ppm.

Analysis of treated water via HPLC confirmed the absence of phenol or release of its derivatives, such as p-hydroxybenzoic acid, hydroquinone, catechol and protocatechuate (Tao et al., 2005; Martínková et al., 2009). A few peaks with retention times in the range of 1 & 2 min were observed which most probably relate to the peak of the solvent, or to the final degradation products of phenol, possibly tri-carbonic acids. The biodegradation of *p*-cresol

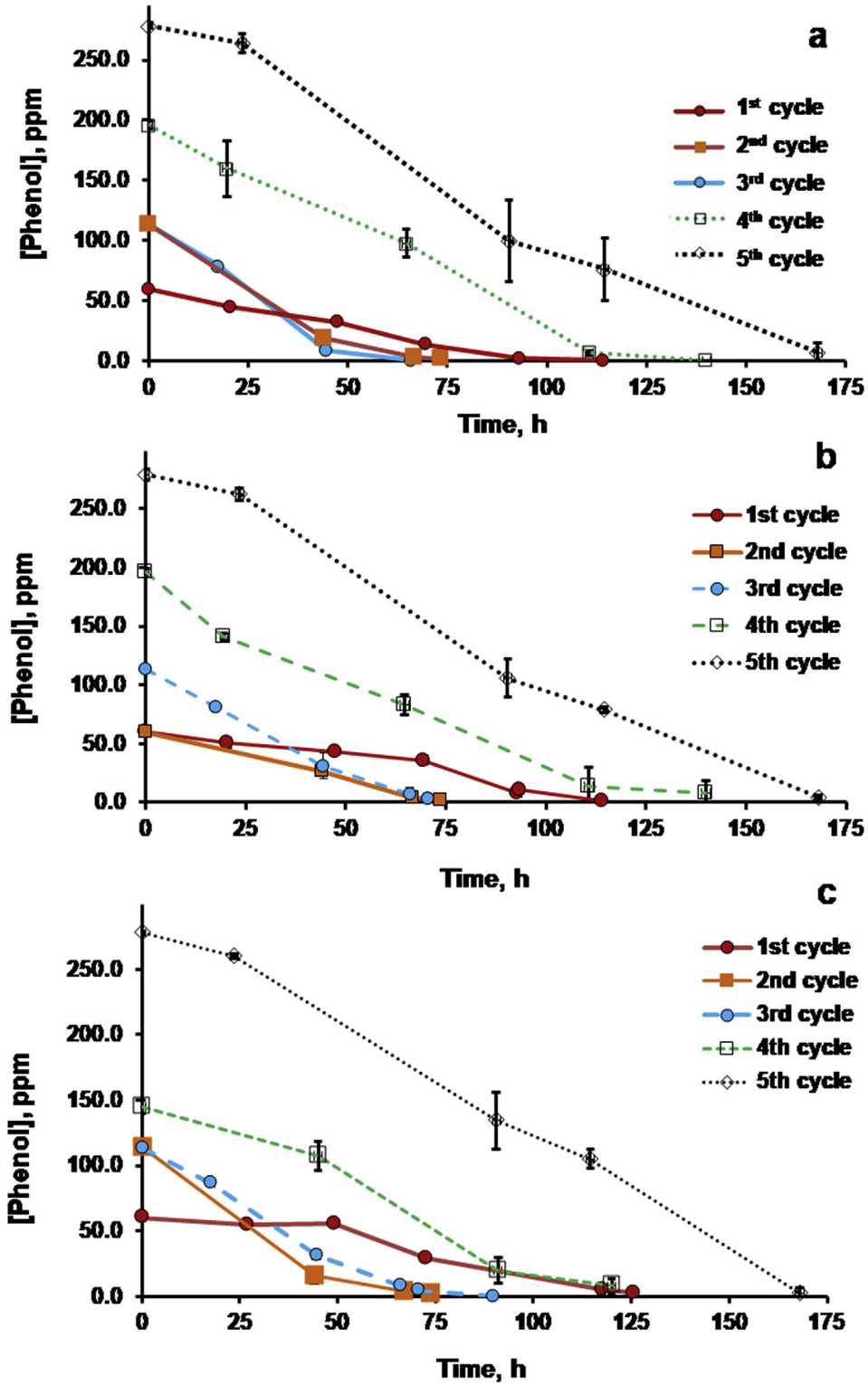

Fig. 5. Degradation of phenol in MSM by CBRs in plastic ("Kaldnes") carriers: A) CBR-*Pse* (total cell number $12.2 \pm 3.6 \times 10^6$ CFU); B) CBR-*Acn*, ($29.7 \pm 1.42 \times 10^6$ CFU); C) CBR-*Rho*, ($2088 \pm 99 \times 10^6$ CFU). Two plastic carriers were used in each bottle, phenol solution was 200 mL and concentration: 1st cycle 60 ppm, 2nd and 3rd cycles 100 ppm, 4th cycle 200 ppm and 5th cycle 300 ppm (n = 3). Degradation in the first cycle is slower, due to an acclimatisation period of the bacteria to the contaminant.

performed using suspensions of *Pse* and *Rho* revealed a trace amount of *p*-cresol, and some trace amounts of its derivatives were detected after 2 weeks of bioremediation by suspensions of bacteria *Pse*, *Rho* and the corresponding cryobacteria reactors. The bioremediation results for *p*-cresol and m-cresol were comparable. Indirect evidence of the release of tri-carbonic acids was given by a pH shift from 7.1 to 6.5–6.4 which is in agreement with previously described pathways of degradation of phenols and cresols (Kolomytseva et al., 2007).

Table 2
Number of viable cells in initial cryogel and after 10, 28 and 40(*) days of the bioremediation process (n = 3) estimated using MTT assay. CBR-*Pse* control (without contaminant) the number of cells was 18.9 ± 2.5 × 10^6 CFU after 10 days in MSM at 4 °C.

Contaminant concentration and volume	Before remediation.	2CP, 40 mL, 50 ppm	m-cresol, 40 mL, 50 ppm	m-cresol, 40 mL 100 ppm	Phenol, 200 mL, 300 ppm
Time point, days	0	10	10	10	28
Number of viable cells x 10^6					
CBR-*Acn*	39.7 ± 1.42	10.4 ± 3.12		–	17.6 ± 0.96
CBR-*Pse*	12.2 ± 3.64	–	34 ± 2.54	–	38.1 ± 8.3
CBR-*Rho*	2088 ± 99	653 ± 64	716 ± 122	453 ± 105	576 ± 52
Cryo-RhoGel 1.0% *	–	70.46 ± 18.6	–	–	–
Cryo-RhoGel 0.5%*	–	76.0 ± 5.5	–	–	–
Cryo-PseGel 0.5% *	–	82.1 ± 10.8	–	–	–
Cryo-PseGel 1.0%*	–	60.8 ± 3.4	–	–	–
Pse suspension *	–	46.8 ± 8.8	–	–	–

3.3. Biodegradation of chlorophenols

Chlorophenols (CPs) are relatively stable products of the biodegradation of triclosan and triclocarban, which are widely used as antimicrobial agents in toothpaste, soaps and detergents and are present in most waste waters (Dhillon et al., 2015). Therefore, the efficiency of the developed Cryo-*Rho*, Cryo-*Pse*, Cryo-*Acn* reactors for degrading various CPs was examined. The viability of bacteria via monitoring of turbidity as well as their biodegradation efficiency for 4CP and 2CP in carbonate buffer and minimum salt media (MSM) at pH 7.2 was estimated (Figs. S7 and S9). Data indicated that bioremediation efficiency for suspensions of *Acn*, *Rho* and *Pse* were negligible (40 mL 50 ppm 4CP) in carbonate buffer at 48 and 120 h, respectively. Bioremediation efficiencies for suspension of the *Rho* and *Pse* in MSM were 0.044 ± 0.019 mg/L/h and 0.032 ± 0.025 mg/L/h (40 mL 50 ppm 4CP) at 48 and 220h, respectively (Fig. S8). From the cryobacteria reactors tested, only cryo-*Pse* PVA-al or PVA-al-PEI-al showed consistent ability to degrade 4CP (Fig. 6 and Table 1), although cryo-*Rho* showed some degradative.

The 4CP degradation efficiency was much lower compared to bioremediation efficiencies for phenol or m-cresol using the same bacterial strains. Biodegradation of 2CP (60 ppm) resulted in only a 9% decrease after 6.6 days (Table S2). Control cryogels of PEI-al-PVA-al and PVA-al (without bacteria) did not reveal adsorption of phenols or CPs or self-decomposition of the contaminant within 1000h of incubation in the 4-CP (50 ppm) solution (40 mL).

One can observe that Gel based cryogels cross-linked by magnesium ions were less efficient in the bioremediation process compared to sodium cross-linked physical gel, which may be related to some diffusion restriction, as Gel forms a hydrogel such faster. Estimation of the final concentration of 4CP was performed using HPLC, illustrating that suspensions of bacteria (*Pse and Rho*) and cryo-*Pse* and cryo-*Rho* can slowly degrade 4CP (Table S2, Fig. 6). It was observed that *Rho* immobilized within the cryogel structure is capable of degrading chlorophenol without additional sources of carbon. These data indicate that cryo-*Pse* and cryo-*Rho* bioreactors, while less effective for 4CP and 2CP, warrant further study in their application for treatment of waste water from hospitals, which has high concentrations of recalcitrant chlorophenols and their metabolites which require removal.

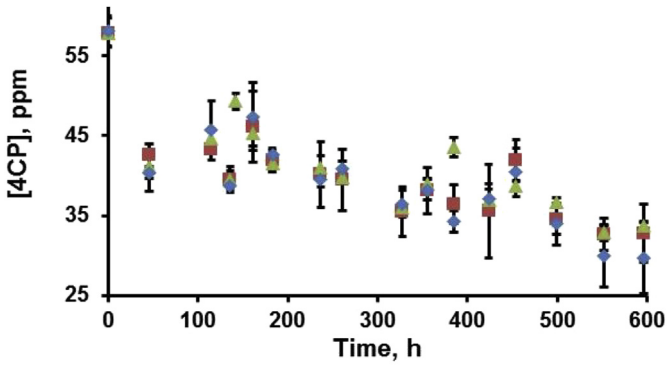

Fig. 6. Degradation of 4CP in MSM (50 ppm 40 mL) by cryogel made of: (■) cryo-*Pse*-Gel-Mg(1.0%), (◆) cryo-*Pse*-Gel-Mg(0.5%), (▲) cryo-*Pse*-Gel-Na(1%), (O) cryo-*Pse*-Gel-Na(0.5%), (Δ) cryo-*Rho*-Gel-Na(0.5%), (●) cryo-*Rho*-Gel-Na(1.0%), (n = 3) dynamic mode, 2.9 ± 0.12 E7 CFU of cells per cryogel; cryo-*Pse* with approximate the same amount of cells in each cryogel: (◆)1.7% PVA-al; (■) PVA-al-PEI-al(0.35: 0.55%); (▲) PVA-al-PEI-al 0.5:0.6% (Cryo-*Pse*), (n = 2).

4. Conclusion

3D structured bioreactors based on live bacteria, suitable for the bioremediation of a range of phenol derivatives (phenol, cresols, chlorophenols), were prepared by cryogelation in a one-step process, using water as a solvent. The macroporous material consisted of 11.6% live bacteria, 1.2% polymers and 87% voids/pores. For the first time toxicity levels of novel aldehyde containing polymers – cross-linking agents (PEI-al and PVA-al) were estimated and their suitable combination proposed. The cryobacteria reactors maintain their degradation activity over at least 10 cycles. The efficiencies of cryobacteria reactors of *Pse, Rho* and *Acn* for degradation of four concentrations of phenol derivatives revealed complete, rapid, bioremediation in dynamic as well as static mode. Moreover, the developed material exhibited significantly better performance for phenol degradation than recently reported by our group, where the bioremediation of 50 ppm of phenol(40 mL) in a dynamic mode was studied (Al-Jwaid et al., 2018). Bioremediation cycles (2^{nd}-10th cycle) were completed within 2.6 days, compared to about 10 days for equivalent cell suspensions. The purification of 200 mL of 300 ppm of phenol by *Pse, Rho and Acn* within cryobacteria reactors took approximately 7 days. The use of plastic carriers showed slightly slower bioremediation of cresols compared to conventional cryobacteria reactors. Overall, six polymers and their combinations were utilised to produce materials for bioremediation purposes using three bacterial strains, the activities of which were tested using four model phenol derivatives. The developed technology preserves the native structure and activity of the bacteria. Cryobacteria reactors have several advantages. Cryogels based on live bacteria can be easily reprocessed after inactivation due to low content of a polymeric cross-linker (<10%) in the structure and therefore the technology can be considered as “green”. There is no diffusion restriction as materials are macroporous with well-developed connected micro channels that improve interaction of the cells with contaminated water. The macroporous structure of interconnected pores also creates the possibility of exploiting the

bioreactor as a flow through column or filter system with no requirement to separate the bacteria after the bioremediation process. The technique is faster and simpler than a previously published three-step cryogel surface immobilisation techniques for phenol degrading bacteria, which also contain a large bulk content of polymer resulting in more complex processing after use.

Acknowledgements

This project received funding from the Marie Skłodowska-Curie grant “Cryo-bacteria-reactor” 701289. The authors are grateful to Dr. Yishan Zheng (UoB, Brighton, UK) and Ing. Miroslav Bačik (Environcentrum s. r.o, Slovakia) for help with HPLC analysis and Areej K.Al-Jwaid (SET, UoB, Brighton, UK) for help with SEM analysis.

Appendix A. Supplementary data

Supplementary data to this article can be found online at https://doi.org/10.1016/j.watres.2019.01.028.

References

Al-Jwaid, A.K., Berillo, D., Savina, I.N., Cundy, A.B., Caplin, J.L., 2018. One-step formation of three-dimensional macroporous bacterial sponges as a novel approach for the preparation of bioreactors for bioremediation and green treatment of water. RSC Adv. 8 (54), 30813–30824. https://doi.org/10.1039/C8RA04219E.

Anku, W.W., Mamo, M.A., Govender, P.P., 2017. Phenolic Compounds in Water: Sources, Reactivity, Toxicity and Treatment Methods. Phenolic Compounds-Natural Sources, Importance and Applications. InTech. https://doi.org/10.5772/66927.

Berillo, D., Volkova, N., 2014. Preparation and physicochemical characteristics of cryogel based on gelatin and oxidised dextran. J. Mater. Sci. 49 (14), 4855–4868. https://doi.org/10.1007/s10853-014-8186-3.

Börner, R.A., Zaushitsyna, O., Berillo, D., Scaccia, N., Mattiasson, B., Kirsebom, H., 2014. Immobilization of Clostridium acetobutylicum DSM 792 as macroporous aggregates through cryogelation for butanol production. Process Biochem. 49 (1), 10–18. In: https://doi.org/10.1016/j.procbio.2013.09.027.

Chen, Y.-M., Lin, T.-F., Huang, C., Lin, J.-C., Hsieh, F.-M., 2007. Degradation of phenol and TCE using suspended and chitosan-bead immobilized Pseudomonas putida. J. Hazard Mater. 148 (3), 660–670.

Chiellini, E., Corti, A., Solaro, R., 1999. Biodegradation of poly(vinyl alcohol) based blown films under different environmental conditions Part of work herewith reported was presented at the 5th Scientific Workshop on Biodegradable Polymers and Plastics, Stockholm (Se) June 1998. Polym. Degrad. Stabil. 64 (2), 305–312. https://doi.org/10.1016/S0141-3910(98)00206-7.

Cortez, S., Nicolau, A., Flickinger, M.C., Mota, M., 2017. Biocoatings: A new challenge for environmental biotechnology. Biochem. Eng. J. 121 (Suppl. C), 25–37. https://doi.org/10.1016/j.bej.2017.01.004.

Dhillon, G.S., Kaur, S., Pulicharla, R., Brar, S.K., Cledón, M., Verma, M., Surampalli, R.Y., 2015. Triclosan: current status, occurrence, environmental risks and bioaccumulation potential. Int. J. Environ. Res. Publ. Health 12 (5), 5657–5684. https://doi.org/10.3390/ijerph120505657.

Dzionek, A., Wojcieszyńska, D., Guzik, U., 2016. Natural carriers in bioremediation: a review. Electr. J. Biotechnol. 19 (5), 28–36. https://doi.org/10.1016/j.ejbt.2016.07.003.

El-Naas, M.H., Al-Muhtaseb, S.A., Makhlouf, S., 2009. Biodegradation of phenol by Pseudomonas putida immobilized in polyvinyl alcohol (PVA) gel. J. Hazard Mater. 164 (2), 720–725. https://doi.org/10.1016/j.jhazmat.2008.08.059.

Gonzalez, G., Herrera, G., Garcı, M.T., Pena, M., 2001. Biodegradation of phenolic industrial wastewater in a fluidized bed bioreactor with immobilized cells of Pseudomonas putida. Bioresour. Technol. 80 (2), 137–142. https://doi.org/10.1016/S0960-8524(01)00076-1.

Hailei, W., Ping, L., Yu, Q., Hui, Y., 2016. Removal of phenol in phenolic resin wastewater by a novel biomaterial: the Phanerochaete chrysosporium pellet containing chlamydospore-like cells. Appl. Microbiol. Biotechnol. 100 (11), 5153–5164. https://doi.org/10.1007/s00253-016-7353-7.

Hao, O.J., Kim, M.H., Seagren, E.A., Kim, H., 2002. Kinetics of phenol and chlorophenol utilization by Acinetobacter species. Chemosphere 46 (6), 797–807. https://doi.org/10.1016/S0045-6535(01)00182-5.

Kirsebom, H., Mattiasson, B., Galaev, I.Y., 2009. Building macroporous materials from microgels and microbes via one-step cryogelation. Langmuir 25 (15), 8462–8465. https://doi.org/10.1021/la9006857.

Kirsebom, H., Elowsson, L., Berillo, D., Cozzi, S., Inci, I., Piskin, E., Galaev, I.Y., Mattiasson, B., 2013. Enzyme-catalyzed crosslinking in a partly frozen state: a new way to produce supermacroporous protein structures. Macromol. Biosci. 13 (1), 67–76. https://doi.org/10.1002/mabi.201200343.

Kolomytseva, M.P., Baskunov, B.P., Golovleva, L.A., 2007. Intradiol pathway of para-cresol conversion by Rhodococcus opacus 1CP. Biotechnol. J. 2 (7), 886–893. https://doi.org/10.1002/biot.200700013.

Martínková, L., Uhnáková, B., Pátek, M., Nešvera, J., Křen, V., 2009. Biodegradation potential of the genus Rhodococcus. Environ. Int. 35 (1), 162–177. https://doi.org/10.1016/j.envint.2008.07.018.

Milović, N.M., Wang, J., Lewis, K., Klibanov, A.M., 2005. Immobilized N-alkylated polyethylenimine avidly kills bacteria by rupturing cell membranes with no resistance developed. Biotechnol. Bioeng. 90 (6), 715–722. https://doi.org/10.1002/bit.20454.

Önnby, L., Giorgi, C., Plieva, F.M., Mattiasson, B., 2010. Removal of heavy metals from water effluents using supermacroporous metal chelating cryogels. Biotechnol. Prog. 26 (5), 1295–1302. https://doi.org/10.1002/btpr.422.

Rusten, B., Eikebrokk, B., Ulgenes, Y., Lygren, E., 2006. Design and operations of the Kaldnes moving bed biofilm reactors. Aquacult. Eng. 34 (3), 322–331.

Satchanska, G., Topalova, Y., Dimkov, R., Groudeva, V., Petrov, P., Tsvetanov, C., Selenska-Pobell, S., Golovinsky, E., 2015. Phenol degradation by environmental bacteria entrapped in cryogels. Biotechnol. Biotechnol. Equip. 29 (3), 514–521. https://doi.org/10.1080/13102818.2015.1009167.

Sinha, P.K., Sinha, A., Das, M., 2011. Microbial removal of phenol and p-chlorophenol from industrial waste water using Rhodococcus sp. RSP8 and its growth kinetic modeling. J. Water Resour. Protect. 3 (08), 634. https://doi.org/10.4236/jwarp.2011.38073.

Tao, Y., Fishman, A., Bentley, W.E., Wood, T.K., 2004. Altering toluene 4-monooxygenase by active-site engineering for the synthesis of 3-methoxycatechol, methoxyhydroquinone, and methylhydroquinone. J. Bacteriol. 186 (14), 4705–4713. https://doi.org/10.1128/JB.186.14.4705-4713.2004.

Tao, Y., Bentley, W.E., Wood, T.K., 2005. Phenol and 2-naphthol production by toluene 4-monooxygenases using an aqueous/dioctyl phthalate system. Appl. Microbiol. Biotechnol. 68 (5), 614–621. https://doi.org/10.1007/s00253-005-1939-9.

Villegas, L.G.C., Mashhadi, N., Chen, M., Mukherjee, D., Taylor, K.E., Biswas, N., 2016. A short review of techniques for phenol removal from wastewater. Curr. Pollut. Rep. 2 (3), 157–167. https://doi.org/10.1007/s40726-016-0035-3.

Virgen-Ortíz, J.J., dos Santos, J.C., Berenguer-Murcia, Á., Barbosa, O., Rodrigues, R.C., Fernandez-Lafuente, R., 2017. Polyethylenimine: a very useful ionic polymer in the design of immobilized enzyme biocatalysts. J. Mater. Chem. B 5 (36), 7461–7490. https://doi.org/10.1039/C7TB01639E.

Zaushitsyna, O., Berillo, D., Kirsebom, H., Mattiasson, B., 2014. Cryostructured and crosslinked viable cells forming monoliths suitable for bioreactor applications. Top. Catal. 57 (5), 339–348. https://doi.org/10.1007/s11244-013-0189-9.